journal

J. Am. Ceram. Soc., 84 [3] 561–65 (2001)

Brittle Fracture versus Quasi Plasticity in Ceramics: A Simple Predictive Index

Young-Woo Rhee,† Hae-Won Kim,‡ Yan Deng,§ and Brian R. Lawn*

Materials Science and Engineering Laboratory,
National Institute of Standards and Technology, Gaithersburg, Maryland 20899

Simple relations for the onset of competing brittle and quasi-plastic damage modes in Hertzian contact are presented. The formulations are expressed in terms of well-documented material parameters, elastic modulus, toughness, and hardness, enabling *a priori* predictions for given ceramics and indenter radii. Data from a range of selected ceramic (and other) materials are used to demonstrate the applicability of the critical load relations, and to evaluate coefficients in these relations. The results confirm that quasi plasticity is highly competitive with fracture in ceramics, over a sphere radius range 1–10 mm. Implications concerning the brittleness of ceramics in the context of indentation size effects are discussed.

I. Introduction

RECENT studies using Hertzian contact with spheres have identified two basic damage modes in monolithic ceramics:[1–7] *brittle mode*, consisting of tension-driven Hertzian cone cracks in the top surface; *quasi-plastic mode*, consisting of a "yield" zone of distributed shear-driven faults or microcracks in the subsurface. The latter mode is especially prominent in indentation fields, especially in "sharp" contacts, because of an uncommonly high shear/tension stress ratio, typically 2 or more[8] (see Section II). It is therefore important to give due consideration to this mode in any ceramics application involving concentrated loading, e.g., bearings, dental crowns.[7,9] Cone cracks have been well studied using conventional fracture mechanics[7,10–18] and dominate in hard ceramics with single-valued toughness. Quasi plasticity is less well understood, requiring micromechanical damage accumulation descriptions,[19,20] and occurs more readily in tough ceramics with *R*-curves. Both modes can be strength degrading,[21] but quasi plasticity is particularly damaging in fatigue and wear applications,[1,7,22,23] from cumulative microcrack coalescence.

Hertzian testing can be used to measure the relative loads for the onset of each damage mode in any specified material, at any given indenter radius.[7] However, such measurements may not always be straightforward. If the material is opaque, one usually has to examine the specimen after the indentation events, using exacting surface microscopy or painstaking sectioning techniques. Even instrumented force–displacement indentation tests,[24] so useful in quantifying hardness, do not generally have the necessary sensitivity to detect the very first initiation of inelastic damage beneath spherical indenters on brittle materials.[25] Acoustic emission also is limited in its ability to detect individual damage events, particularly the microscopic shear events which characterize the quasi plasticity initiation process—in some materials associated microcracks grow relatively stably with increasing (sometimes decreasing) contact load,[19] and are therefore unlikely to emit detectable signals. It would therefore appear desirable to be able to predict critical loads *a priori*, using routinely available, basic material properties.

Accordingly, in this study we present simple relations for the critical loads for quasi plasticity and cone fracture in Hertzian contact, in terms of elastic modulus, toughness, and hardness. The underlying formalism for this purpose is well established in the indentation literature.[26–33] We demonstrate the applicability of the formulations by measuring critical loads for the onset of quasi plasticity and cone fracture on a broad range of selected ceramic materials. Our results indicate that quasi plasticity is highly competitive with fracture in most ceramics, over a sphere-radius test range 1–10 mm. The analysis confirms an indentation size effect in which quasi plasticity dominates at small characteristic indentation dimensions and fracture dominates at large dimensions.

II. Critical Loads for Quasi Plasticity and Fracture

Figure 1 shows a schematic of a surface-initiated cone crack and subsurface-initiated quasi-plastic deformation zone for indentation of a flat specimen of Young's modulus E with a sphere of radius r at load P. The material is assumed to remain elastic up to the onset of first damage, so that the contact may be described by the classical Hertzian field. A general relation for the contact radius is[8]

$$a = \{3(1 - \nu^2) Pr'/4E'\}^{1/3} \tag{1}$$

with ν Poisson's ratio (here taken as approximately equal for indenter and specimen) and with r' "effective radius" and E' "effective modulus"

$$1/r' = 1/r + 1/r_s \tag{2a}$$

$$1/E' = 1/E + 1/E_i \tag{2b}$$

where subscripts s and i denote specimen surface and indenter material, respectively. This formulation allows us to account for indenters of different modulus and specimens of different curvature. Thus for rigid indenters on flat specimens, $r' = r$ and $E' = E$; whereas for like indenters and specimens, $r' = r/2$ and $E' = E/2$. (Note that the contact radius a in Eq. (1) is the same for these two illustrative cases.)

For the quasi-plastic mode, it is assumed that damage is driven by the shear component of the Hertzian stress field.[34,35] The shear stress has a maximum value just under one half the mean indentation pressure, $\tau_m \approx 0.47\ P/\pi a^2$, at a subsurface location along the contact axis.[8,34] Yield initiates when τ_m reaches one half the uniaxial yield stress, $\tau_m \approx Y/2$.[1,7,34,36–38] The yield stress can be related to the indentation hardness H via the simple relation $H = cY$, where c is a "constraint factor"—for ideal elastic–plastic

D. B. Marshall—contributing editor

Manuscript No. 188500. Received June 6, 2000; approved October 4, 2000.
Supported by grants from the Korea Science and Engineering Foundation (Y.-W. Rhee) and the U.S. National Institute of Dental Research.
*Member, American Ceramic Society.
†Ph.D. student, Department of Materials Science and Engineering, Korea Advanced Institute of Science and Technology, Yusong, Taejon 305-701, Korea.
‡Ph.D. student, School of Materials Science and Engineering, Seoul National University, Seoul 1512-742, Korea.
§Ph.D. student, Department of Materials and Nuclear Engineering, University of Maryland, College Park, Maryland 20742.

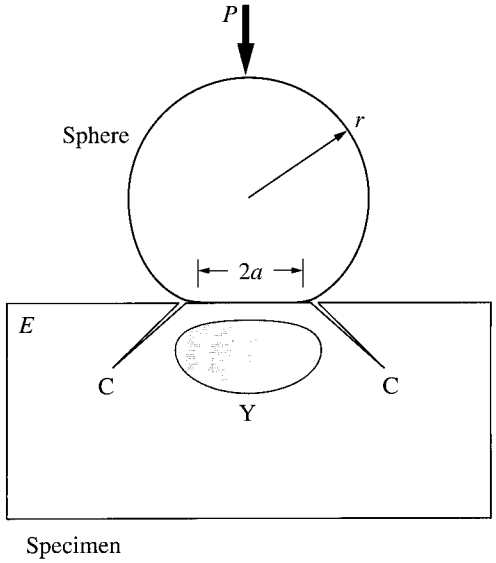

Fig. 1. Schematic showing competing damage modes in ceramic specimen from contact with sphere indenter: *brittle mode*, cone crack (C); *quasi-plastic mode*, yield zone (Y).

Table I. Material Parameters†

Material	Young's modulus E (GPa)	Hardness H (GPa)	Toughness T (MPa · $m^{1/2}$)	Ref.
Polycrystalline ceramics				
Soda-lime glass‡	70	5.2	0.67	41
Porcelain‡	68	6.2	0.92	42
Glass-ceramic (Dicor)‡	69	3.8	1.2	
Glass-ceramic (Macor)‡	63	2.5	1.9	
F-MGC‡	71	3.8	1.0	43
M-MGC‡	67	3.2	1.3	43
C-MGC‡	50	2.5	1.7	43
Al_2O_3 (AD999)‡	390	17.5	3.1	
Al_2O_3 (Glass-infiltrated)‡	271	12.3	2.7	44
ZrO_2 (Y-TZP)‡	205	12.0	5.4	23
F-Si_3N_4	335	21.0	3.9	6
M-Si_3N_4	326	17.9	5.3	6
C-Si_3N_4	315	15.8	6.0	6
Other materials				
Diamond	1000	80	4.0	31
Silicon	170	14	0.70	31
WC	614	16	13	35
Mild steel	210	1.1	50	35
Polycarbonate‡	2.3	0.14	2	45

†Uncertainties in E estimated at ≈5%, H ≈10%, and T ≈20%. ‡Materials for which supplementary data were obtained.

solids, $c \approx 3$.[34] Combining these relations with Eq. (1) provides an expression for the critical contact load P_Y at first yield:[30]

$$P_Y/r'^2 = DH(H/E')^2 = \text{constant} \quad (3)$$

with $D = (1.1\pi/c)^3[3(1 - \nu^2)/4]^2$ a dimensionless constant.

The brittle mode is driven by the tensile component of the Hertzian field. The maximum tensile stress is $\sigma_m = (1 - 2\nu)P/2\pi a^2$ at the circle of contact, but falls off dramatically below the top surface.[10] The ensuing cone crack accordingly undergoes a complex stabilized growth stage *en route* to pop-in. The condition for crack initiation is that the stress intensity factor $K(C) = \sigma_m(\pi C)^{1/2}F(C/a) = T$, $dT/dC > 0$, where C is crack length and $T = K_{IC}$ is toughness (assumed single-valued). The corresponding critical load is thus determined as[7,10,12,13,15,31,39,40]

$$P_C/r' = AT^2/E' = \text{constant} \quad (4)$$

which is Auerbach's law, with $A = A(\nu)$. Unlike D in Eq. (3), A is not amenable to accurate first-principles evaluation, and is best obtained by experimental calibration.

We note that $\tau_m/\sigma_m \approx 0.47/0.5(1 - 2\nu) \approx 2$, as indicated in Section I. We note also the different critical load dependence on indenter radius r' in these relations, quadratic in Eq. (3) and linear in Eq. (4). These different dependencies have been well documented in the literature cited above.

III. Experimental Procedure

Several polycrystalline ceramic materials was selected for the present study, as listed in Table I. These materials were chosen because their mechanical properties had been well characterized in previous studies, and because the range of material parameters was sufficiently broad to ensure meaningful data trends. Among these ceramics were series of micaceous glass-ceramics (MGCs), aluminas, and silicon nitrides, distinguished by fine (F), medium (M), and coarse (C) microstructures. Some additional materials, diamond-type single crystals and soda–lime glass at the brittle end, and representative metals and polymers at the plastic end, were included for subsequent comparison purposes.

Specimens were cut into bars with minimum surface dimension 5 mm and minimum thickness 3 mm. Surfaces of the polycrystalline ceramics were polished to 1 μm finish. These materials had a sufficiently dense population of intrinsic microstructural flaws to ensure crack initiation in the ensuing contact tests. The soda–lime glass surfaces were lightly abraded with 600 SiC grit, to provide an adequate density of extrinsic flaws.[46]

In those materials where values of elastic modulus, hardness, and toughness values were not available from previous studies, supplementary measurements were made using routine testing procedures. Elastic modulus was determined by a sonic method (Grindosonic MK5, J. W. Lemmens Inc., St. Louis, MO). Hardness and toughness were determined by Vickers indentation (Zwick 3212, Zwick USA, Kennesaw, GA) over a load range 10–100 N: indentation hardness as $H = 2P/d^2$ (load/projected area),[34] with d impression diagonal (converting any Vickers hardness numbers using $H = 1.078H_V$); and indentation toughness, $T = 0.016(E/H)^{1/2}(P/c^{3/2})$,[47] with c radial crack length measured from the contact center. Measurements of d and c were made 1 h after indentation. Any such supplementary determinations are indicated by asterisk in Table I.

Hertzian contact tests were made on the prepared ceramic and glass surfaces, using WC spheres within a radius range r = 1–10 mm fixed into the crosshead of an Instron testing machine (Model 1122, Instron Corp., Canton, MA), at a loading rate of 0.2 mm·min^{-1}, in air. Indentations were made in rows on each specimen surface at designated load increments, for each given ball size. After the indented surfaces were gold-coated, critical loads were determined by optical microscopy using Nomarski interference contrast—a postcontact gold coating usefully enhanced image contrast. All observations were made within 1 h of indentation. Means and uncertainty bounds for P_Y were determined from the load ranges over which residual surface impressions were completely undetectable (lower limit) and were clearly visible (upper limit). In Y-TZP, these impressions showed a marked tendency to recovery after several hours, disappearing altogether for loads just above threshold—in this material, a special effort was made to observe the indentation sites within 5 min of indentation. Analogous limits for P_C were determined from the load ranges over which the cone cracks first appeared on the surfaces as incipient shallow arcs and finally completed themselves as full surface rings around the contact. In some materials (e.g., the glass-infiltrated alumina) this spread was relatively large. In the more brittle ceramics (glass, porcelain) it was difficult to produce any visible quasi-plastic deformation at loads less than $\approx 3P_C$; conversely, in the more quasi-plastic ceramics (coarser glass-ceramics and silicon nitrides), it was difficult to produce cone cracks below $\approx 3P_Y$. In some of the intermediate cases, both modes were apparent within these load ranges.

IV. Data Analysis

Critical load data are plotted as P_Y/r'^2 versus $H(H/E')^2$ for quasi plasticity in Fig. 2 and as P_C/r' versus T^2/E' for cone fracture in Fig. 3, in accordance with Eqs. (3) and (4). Each data point represents mean values over all measurements for a given material, within the range $r = 1$–10 mm. Vertical error bars are standard deviations of the experimental P_Y and P_C measurements; horizontal error bars represent bounds from composite uncertainties in material parameters E (nominal 5%), H (10%), and T (20%).[47] Note the wide range of critical loads covered by the data. Softer/tougher materials (metals, polymers) tend to the lower end of the range in Fig. 2, and to the upper end (off scale) in Fig. 3.

The solid lines in Figs. 2 and 3 are best fits of Eqs. (3) and (4) to the data. We exclude some of the data from these fits: for the quasi plasticity mode in Fig. 2, data for the harder materials, $H > H_{WC}$ (e.g., silicon nitrides[6]), where flattening of the WC spheres tends to produce artificially high values of P_Y; for the brittle mode in Fig. 3, data for $P_C > 2P_Y$, since precursor quasi plasticity can redistribute the tensile stresses. The resulting fits yield values for the respective coefficients: for the quasi-plastic mode, $D = 0.85$ (cf. $D = 0.75$ calculated directly from Eq. (3), for $c = 3$, $\nu = 0.25$); for the fracture mode, $A = 8.6 \times 10^3$ (cf. $A = 2$–3×10^3 for $\nu = 0.25$ from previous investigators[15,39]). Note that the data points for some of the materials do not intersect the fitted lines, indicating some systematic deviations.

V. Discussion

We have used a simple, well-documented formulation for quantifying competing damage modes, brittle fracture, and quasi plasticity, at Hertzian contacts in ceramics, with due allowance for the elastic deformability of the indenter and curvature of the specimen. Specifically, we have presented explicit relations for the critical loads P_C and P_Y in terms of basic material parameters: for quasi plasticity, hardness (H), and modulus (E); for brittle fracture, toughness ($T = K_{Ic}$) and modulus (E). Experimental determinations of the critical loads in selected ceramic materials (Table I) have been used to best-fit proportionality coefficients in these relations. With these coefficients thus determined, we have the basis for *a priori* predictions of critical loads for any other given ceramic material from E, H, and T values, foregoing the need for direct, often exacting, experimental determinations.

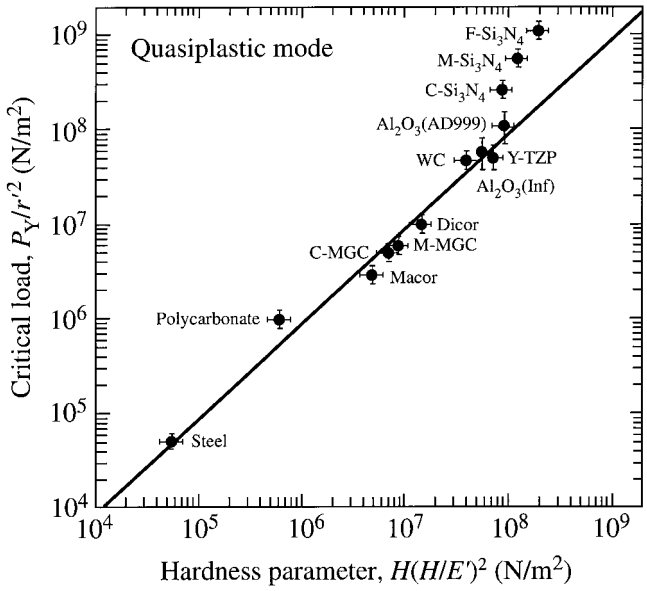

Fig. 2. Critical load quantity P_Y/r'^2 for onset of quasi plasticity in selected materials, as a function of parameter $H(H/E')^2$. Vertical error bar is experimental mean and standard deviation; horizontal error bar is nominal uncertainty from hardness and modulus values. Solid line is best fit to Eq. (3), corresponding to $D = 0.848$.

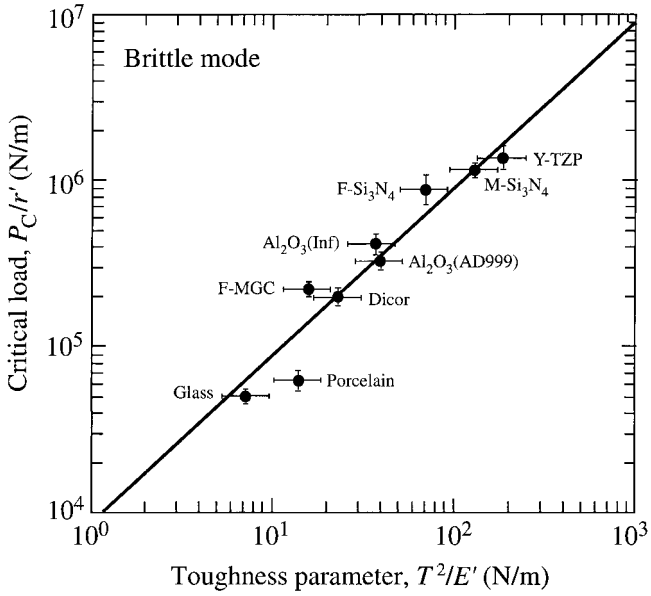

Fig. 3. Critical load quantity P_C/r' for onset of cone cracking in selected materials, as a function of parameter T^2/E'. Vertical error bar is experimental mean and standard deviation; horizontal error bar is nominal uncertainty from toughness and modulus values. Solid line is best fit to Eq. (4), corresponding to $A = 8.63 \times 10^3$.

As indicated in Section I, the quasi plasticity mode can be at least as deleterious as the brittle mode in strength, fatigue, and wear properties. The proper design of ceramics requires that maximum operational contact loads P_m remain below both P_C and P_Y. While the sizes of individual microcracks within a quasi-plastic zone may appear much smaller than those of cone cracks in brittle materials, at least at first initiation, these same microcracks are prone to coalesce into far more dangerous cracks at high loads and large numbers of cycles:[1,7,22,23] the cumulative effect on strength degradation and material removal processes can then be catastrophic. Yet quasi plasticity ordinarily goes overlooked in conventional tensile testing procedures. In flexural specimens, for instance, the magnitude of the shear component is one half that of the tensile component (i.e., exactly the reverse of the situation in contact fields), in which case quasi plasticity may never be activated. Accordingly, it is not always practical to extrapolate data from tensile test specimens to concentrated-load configurations.

The competition between quasi plasticity and brittle fracture apparent in the Hertzian contact field bears on the issue of brittleness.[26–33] From Eqs. (2) and (3) we have

$$P_Y/P_C = (D/A)(H/E')(H/T)^2 r' \tag{5}$$

which may be taken as a brittleness index for any given contact radius: if $P_Y/P_C > 1$, the response is brittle; if $P_Y/P_C < 1$, it is quasi-plastic. Figure 4 plots calculated P_Y/P_C versus $(H/E')(H/T)^2$ for the ceramic materials in Table I, including diamond, silicon, and glass, for a midrange radius $r' = 3.18$ mm. The data in this figure suggest that quasi plasticity in ceramics may be more prevalent than might ordinarily be expected. The lateral position of the predicted line translates to the left or right as the radius r' decreases or increases, displacing some of the materials from one region to the other. There is the indication of an intrinsic size effect in the competition between quasi-plastic and brittle fracture modes, quantified by the transition point at $P_Y/P_C = 1$, $r' = r_*$ say:[30]

$$r_* = (A/D)(E'/H)(T/H)^2 \tag{6}$$

Such size effects arise because of the different dimensional dependencies of the two modes, with plasticity essentially a volume effect and fracture a surface effect.[31] Figure 5 indicates values of r_* for all materials in Table I (including the relatively

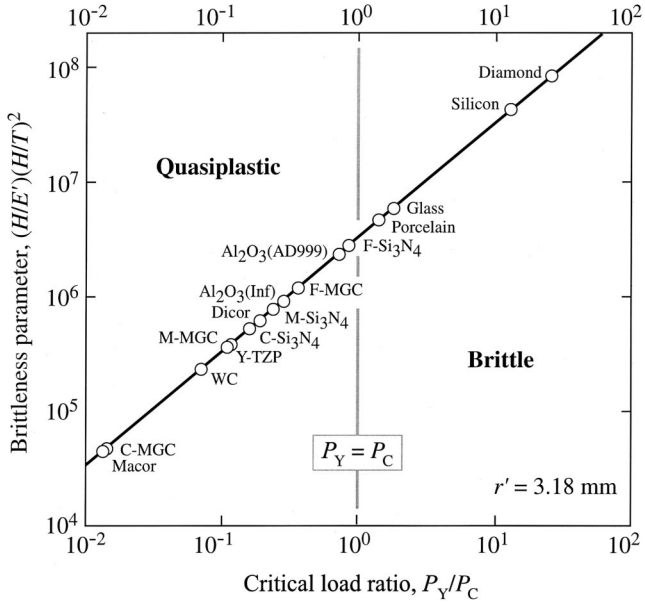

Fig. 4. Calculated critical load ratio P_Y/P_C for ceramics in Table I, for midrange sphere radius $r' = 3.18$ mm on logarithmic plot (relative to test range $r' = 1$–10 mm over which P_Y and P_C data in Figs. 2 and 3 were measured). Materials to right of vertical line $P_Y/P_C = 1$ lie in "brittle" region; those to left lie in "quasi-plastic" region. A decrease or increase in r' scales solid line laterally to left or right, shifting more materials into quasi-plastic or brittle region, respectively.

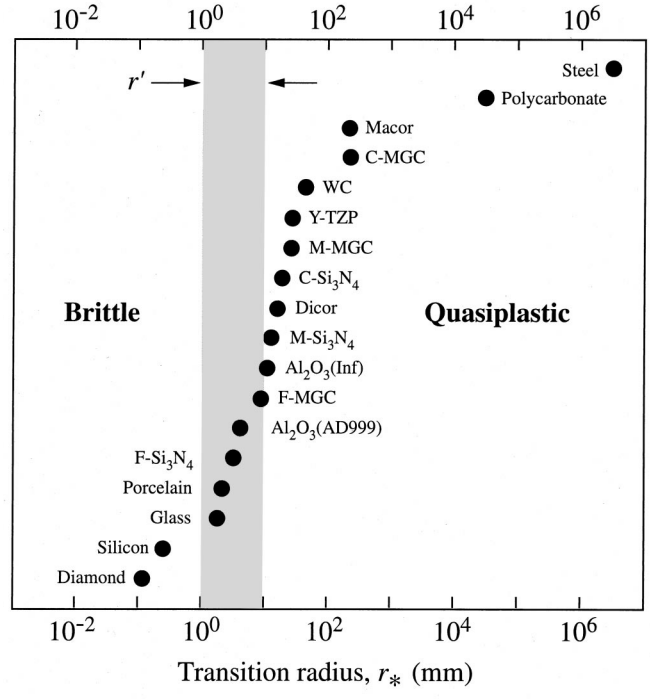

Fig. 5. Transition sphere radius r_* at which critical loads $P_Y = P_C$ for materials in Table I. Ordinate ranks the materials according to increasing r_*. Data points are values calculated from Eq. (5) using materials parameters from Table I. Relative to any operational sphere radius r', region $r_* > r'$ ($P_Y < P_C$) corresponds to dominant quasi-plastic mode, region $r_* < r'$ ($P_Y > P_C$) to brittle mode. Shaded band indicates test range of r' used to obtain the data in Figs. 2 and 3.

plastic metals and polymers)—the ordinate simply ranks the materials according to increasing r_*, the shaded band indicates the range of sphere radii 1–10 mm covered in our experimental data. From this figure, one can predict whether cracking or quasi plasticity will prevail at any given operational radius r': for $r_* > r'$, quasi plasticity dominates; for $r_* < r'$, brittle fracture dominates. In this context, we note that for bearings and dental crowns the operational value of r' typically lies within the range 1–10 mm, i.e., the range covered by our experimental data, whereas in tribological processes the range is considerably smaller, 1–100 μm say.

Again, the competitive nature of the quasi plasticity mode is apparent. It is interesting to note that the relations in Eqs. (5) and (6) for "blunt" indenters are similar to those for "sharp" (e.g., Vickers) indenters in that they contain a common factor H/T.[27,31] However, whereas blunt and sharp indenters may provide similar rankings for materials brittleness, the other factors in these relations are dissimilar, reflecting essential differences in indentation geometry and leading to quite different absolute predictions of critical loads.

In using the simple formulation presented here to predict threshold conditions for damage in ceramics in contact with curved surfaces, it is well to be aware of limitations imposed by experimental errors and uncertainties arising from theoretical assumptions. In evaluating the coefficients D and A in Eqs. (3) and (4) we have made use of experimental measurements of critical loads P_Y and P_C as well as of material parameters E, H, and T. Estimated scatter bounds in these measurements are shown as the error bars in Figs. 2 and 3. Recall also that some of the data points in these figures actually lie outside the scatter bounds, indicating some systematic deviations. Such deviations may arise in part from the difficulty in measuring P_Y and P_C in some of the materials, due to batch-to-batch specimen variations or to ill-defined initiation events (Section III). Part may arise from inadequacies in the analytical derivations of Eqs. (3) and (4) (Section II). The assumption of ideal elastic–plastic solids implicit in the notion of a constraint factor c in Eq. (3) is open to serious question, because the yield zone geometry is generally not material-invariant in ceramics.[35] Equally open to question are some of the assumptions implicit in the fracture mechanics derivation of Eq. (4).[7] We have averaged out Poisson's ratio effects in our equations, and this quantity can have a strong influence in the critical loads, especially in P_C.[13,39,48] Indenter/specimen friction, neglected here, can modify Hertzian stress fields, with consequent influence on P_C.[49] We have used continuum mechanics in our analysis—grain size can be a modifying factor in both quasi plasticity[50] and cone fracture.[6] In coarser, tougher materials with R-curves, it may be more difficult to determine a meaningful single value of toughness (Vickers tends to give midrange values)—indeed, for the toughest materials it may be difficult to generate contact cracks at all. Rate and chemical effects, especially from intrusive moisture, can enhance the damage process, reducing P_Y[22,51] and P_C;[22,51,52] recovery effects (recall Y-TZP, Section III) can act in the opposite direction. Making allowance for all of these factors, it is probably not reasonable to expect that estimates of P_Y and P_C from Eqs. (3) and (4) are accurate to much better than a factor of 2, rising up to a factor of 5 or more in the worst-behaved materials (e.g., upper right of Fig. 2). In this respect the values of the "calibrated" coefficients $D = 0.85$ and $A = 8.6 \times 10^3$ obtained here should be regarded as approximations only. In the context of the comparatively large range of values covered in Figs. 3 and 4 this level of inaccuracy should not constitute a serious limitation, provided an appropriate safety factor is built into design specifications.

References

[1]F. Guiberteau, N. P. Padture, H. Cai, and B. R. Lawn, "Indentation Fatigue: A Simple Cyclic Hertzian Test for Measuring Damage Accumulation in Polycrystalline Ceramics," *Philos. Mag. A*, **68** [5] 1003–16 (1993).

[2]B. R. Lawn, N. P. Padture, H. Cai, and F. Guiberteau, "Making Ceramics 'Ductile'," *Science (Washington, D.C.)*, **263**, 1114–16 (1994).

[3]H. Cai, M. A. S. Kalceff, B. M. Hooks, B. R. Lawn, and K. Chyung, "Cyclic Fatigue of a Mica-Containing Glass-Ceramic at Hertzian Contacts," *J. Mater. Res.*, **9** [10] 2654–61 (1994).

[4]N. P. Padture and B. R. Lawn, "Toughness Properties of a Silicon Carbide with an *In-Situ*-Induced Heterogeneous Grain Structure," *J. Am. Ceram. Soc.*, **77** [10] 2518–22 (1994).

[5]A. C. Fischer-Cripps and B. R. Lawn, "Indentation Stress–Strain Curves for 'Quasi-Ductile' Ceramics," *Acta Mater.*, **44** [2] 519–27 (1996).

[6]S. K. Lee, S. Wuttiphan, and B. R. Lawn, "Role of Microstructure in Hertzian Contact Damage in Silicon Nitride: I, Mechanical Characterization," *J. Am. Ceram. Soc.*, **80** [9] 2367–81 (1997).

[7]B. R. Lawn, "Indentation of Ceramics with Spheres: A Century After Hertz," *J. Am. Ceram. Soc.*, **81** [8] 1977–94 (1998).

[8]K. L. Johnson, *Contact Mechanics*. Cambridge University Press, London, U.K., 1985.

[9]I. M. Peterson, A. Pajares, B. R. Lawn, V. P. Thompson, and E. D. Rekow, "Mechanical Characterization of Dental Ceramics Using Hertzian Contacts," *J. Dent. Res.*, **77** [4] 589–602 (1998).

[10]F. C. Frank and B. R. Lawn, "On the Theory of Hertzian Fracture," *Proc. R. Soc. London*, **A299** [1458] 291–306 (1967).

[11]T. R. Wilshaw, "The Hertzian Fracture Test," *J. Phys. D: Appl. Phys.*, **4** [10] 1567–81 (1971).

[12]B. R. Lawn and T. R. Wilshaw, "Indentation Fracture: Principles and Applications," *J. Mater. Sci.*, **10** [6] 1049–81 (1975).

[13]R. Warren, "Measurement of the Fracture Properties of Brittle Solids by Hertzian Indentation," *Acta Metall.*, **26**, 1759–69 (1978).

[14]H. Matzke and R. Warren, "Hertzian Crack Growth in ThO_2 Observed by Serial Sectioning," *J. Mater. Sci. Lett.*, **1**, 441–44 (1982).

[15]R. Mouginot and D. Maugis, "Fracture Indentation Beneath Flat and Spherical Punches," *J. Mater. Sci.*, **20**, 4354–76 (1985).

[16]R. F. Cook and G. M. Pharr, "Direct Observation and Analysis of Indentation Cracking in Glasses and Ceramics," *J. Am. Ceram. Soc.*, **73** [4] 787–817 (1990).

[17]K. Zeng, K. Breder, and D. J. Rowcliffe, "The Hertzian Stress Field and Formation of Cone Cracks: I, Theoretical Approach," *Acta Metall.*, **40** [10] 2595–600 (1992).

[18]K. Zeng, K. Breder, and D. J. Rowcliffe, "The Hertzian Stress Field and Formation of Cone Cracks: II, Determination of Fracture Toughness," *Acta Metall.*, **40** [10] 2601–605 (1992).

[19]B. R. Lawn, N. P. Padture, F. Guiberteau, and H. Cai, "A Model for Microcrack Initiation and Propagation Beneath Hertzian Contacts in Polycrystalline Ceramics," *Acta Metall.*, **42** [5] 1683–93 (1994).

[20]B. R. Lawn and D. B. Marshall, "Nonlinear Stress–Strain Curves for Solids Containing Closed Cracks With Friction," *J. Mech. Phys. Solids*, **46** [1] 85–113 (1998).

[21]B. R. Lawn, S. K. Lee, I. M. Peterson, and S. Wuttiphan, "A Model of Strength Degradation from Hertzian Contact Damage in Tough Ceramics," *J. Am. Ceram. Soc.*, **81** [6] 1509–20 (1998).

[22]D. K. Kim, Y.-G. Jung, I. M. Peterson, and B. R. Lawn, "Cyclic Fatigue of Intrinsically Brittle Ceramics in Contact with Spheres," *Acta Mater.*, **47** [18] 4711–25 (1999).

[23]Y.-G. Jung, I. M. Peterson, D. K. Kim, and B. R. Lawn, "Lifetime-Limiting Strength Degradation from Contact Fatigue In Dental Ceramics," *J. Dent. Res.*, **79** [2] 722–31 (2000).

[24]J. S. Field and M. V. Swain, "A Simple Predictive Model for Spherical Indentation," *J. Mater. Res.*, **8**, 297–306 (1993).

[25]S. Wuttiphan, A. Pajares, B. R. Lawn, and C. C. Berndt, "Effect of Substrate and Bond Coat on Contact Damage in Zirconia-Based Plasma Coatings," *Thin Solid Films*, **293** [1–2] 251–60 (1997).

[26]B. R. Lawn, T. Jensen, and A. Arora, "Brittleness as an Indentation Size Effect," *J. Mater. Sci.*, **11** [3] 573–75 (1976).

[27]B. R. Lawn and D. B. Marshall, "Hardness, Toughness, and Brittleness: An Indentation Analysis," *J. Am. Ceram. Soc.*, **62** [7–8] 347–50 (1979).

[28]K. E. Puttick, "Energy Scaling, Size Effects and Ductile-Brittle Transitions in Fracture," *J. Phys. D: Appl. Phys.*, **12**, L19–23 (1979).

[29]K. Puttick, "The Correlation of Fracture Transitions," *J. Phys. D: Appl. Phys.*, **13**, 2249–62 (1980).

[30]R. Mouginot, "Blunt or Sharp Indenters: A Size Transition Analysis," *J. Am. Ceram. Soc.*, **71** [8] 658–61 (1988).

[31]B. R. Lawn, *Fracture of Brittle Solids*; Ch. 8. Cambridge University Press, Cambridge, U.K., 1993.

[32]S. J. Sharp, M. F. Ashby, and N. A. Fleck, "Material Response Under Static and Sliding Indentation Loads," *Acta Mater.*, **41** [3] 685–92 (1993).

[33]J. B. Quinn and G. D. Quinn, "Indentation Brittleness of Ceramics: A Fresh Approach," *J. Mater. Sci.*, **32** [16] 4331–46 (1998).

[34]D. Tabor, *Hardness of Metals*. Clarendon, Oxford, U.K., 1951.

[35]A. C. Fischer-Cripps and B. R. Lawn, "Stress Analysis of Contact Deformation in Quasi-Plastic Ceramics," *J. Am. Ceram. Soc.*, **79** [10] 2609–18 (1996).

[36]M. V. Swain and B. R. Lawn, "A Study of Dislocation Arrays at Spherical Indentations in LiF as a Function of Indentation Stress and Strain," *Phys. Status Solidi*, **35** [2] 909–23 (1969).

[37]M. V. Swain and J. T. Hagan, "Indentation Plasticity and the Ensuing Fracture of Glass," *J. Phys. D: Appl. Phys.*, **9**, 2201–14 (1976).

[38]H. Cai, M. A. Stevens Kalceff, and B. R. Lawn, "Deformation and Fracture of Mica-Containing Glass-Ceramics in Hertzian Contacts," *J. Mater. Res.*, **9** [3] 762–70 (1994).

[39]P. D. Warren, "Determining the Fracture Toughness of Brittle Materials by Hertzian Indentation," *J. Eur. Ceram. Soc.*, **15**, 201–207 (1995).

[40]C. Kocer and R. E. Collins, "The Angle of Hertzian Cone Cracks," *J. Am. Ceram. Soc.*, **81** [7] 1736–42 (1998).

[41]S. M. Wiederhorn, "Fracture Surface Energy of Glass," *J. Am. Ceram. Soc.*, **52** [2] 99–105 (1969).

[42]S. Wuttiphan, "Contact Damage and Fracture of Ceramic Layer Structures"; Ph.D. Thesis. University of Maryland, College Park, MD, 1997.

[43]I. M. Peterson, S. Wuttiphan, B. R. Lawn, and K. Chyung, "Role of Microstructure on Contact Damage and Strength Degradation of Micaceous Glass-Ceramics," *Dent. Mater.*, **14**, 80–89 (1998).

[44]Y.-G. Jung, I. M. Peterson, A. Pajares, and B. R. Lawn, "Contact Damage Resistance and Strength Degradation of Glass-Infiltrated Alumina and Spinel Ceramics," *J. Dent. Res.*, **78** [3] 804–14 (1999).

[45]A. G. Atkins and Y.-M. Mai, *Elastic and Plastic Fracture*. Ellis Horwood, Chichester, U.K., 1985.

[46]H. Chai, B. R. Lawn, and S. Wuttiphan, "Fracture Modes in Brittle Coatings with Large Interlayer Modulus Mismatch," *J. Mater. Res.*, **14** [9] 3805–17 (1999).

[47]G. R. Anstis, P. Chantikul, D. B. Marshall, and B. R. Lawn, "A Critical Evaluation of Indentation Techniques for Measuring Fracture Toughness: I. Direct Crack Measurements," *J. Am. Ceram. Soc.*, **64** [9] 533–38 (1981).

[48]B. R. Lawn, T. R. Wilshaw, and N. E. W. Hartley, "A Computer Simulation Study of Hertzian Cone Crack Growth," *Int. J. Fract.*, **10** [1] 1–16 (1974).

[49]K. L. Johnson, J. J. O'Connor, and A. C. Woodward, "The Effect of Indenter Elasticity on the Hertzian Fracture of Brittle Materials," *Proc. R. Soc. London*, **A334**, 95 (1973).

[50]F. Guiberteau, N. P. Padture, and B. R. Lawn, "Effect of Grain Size on Hertzian Contact in Alumina," *J. Am. Ceram. Soc.*, **77** [7] 1825–31 (1994).

[51]S. K. Lee and B. R. Lawn, "Contact Fatigue in Silicon Nitride," *J. Am. Ceram. Soc.*, **82** [5] 1281–88 (1999).

[52]F. B. Langitan and B. R. Lawn, "Effect of a Reactive Environment on the Hertzian Strength of Brittle Solids," *J. Appl. Phys.*, **41** [8] 3357–65 (1970). □